J|A|C|S
COMMUNICATIONS

Published on Web 07/25/2008

# Separating Chemical Shift and Quadrupolar Anisotropies via Multiple-Quantum NMR Spectroscopy

Jason T. Ash, Nicole M. Trease, and Philip J. Grandinetti*

*Department of Chemistry, The Ohio State University, 100 West 18th Avenue, Columbus, Ohio 43210-1173*

Received April 25, 2008; E-mail: grandinetti.org/contact

The exploitation of chemical shift anisotropy (CSA) for probing structure and dynamics has a long history in magnetic resonance spectroscopy.[1] Phosphate-group[2] and base-pair orientations[3] in nucleic acids, phospholipid headgroup interactions,[4] and enantiomers of chiral molecules[5] have all been investigated via CSA. Numerous applications also exist for the study of proteins, including probing hydrogen-bond formation and secondary structure,[6] characterizing rapid internal motions,[7] and analyzing the dynamics[8] and conformations[9] of protein backbones. The applications previously described involve the use of spin-$^1/_2$ nuclei such as $^1$H, $^{13}$C, $^{15}$N, and $^{31}$P. For these nuclei, the CSA can be measured in a variety of ways, including the use of cross-relaxation[10] or liquid-crystalline solvents[11] in solution as well as the analysis of static spectra or magic-angle spinning (MAS) sidebands[1] in solids.

Nearly 70% of NMR-active nuclei have spin $I > {}^1/_2$, and unfortunately, these nuclei exhibit large quadrupolar couplings that render most solution NMR methods for determining CSA ineffective. These couplings also complicate the analysis of solid-state experiments, as spectra must be fit for the principal components of both the chemical-shift and quadrupolar-coupling tensors as well as for their relative orientation.[12–17] While techniques such as SAS[18] and DACSY[19] have shown significant improvement over traditional methods, they do not explicitly separate the CSA from the quadrupolar anisotropy, and thus, determination of the CSA still requires a large number of fit parameters. They also require rapid sample reorientation during the experiment, making them challenging to implement.

Wang et al.[20] proposed a solution for $I = {}^3/_2$ nuclei in an experiment analogous to multiple-quantum magic-angle spinning (MQ-MAS)[21] except that the rotor is oriented at a magic angle for rank-four interactions (70.12°) rather than the magic angle for rank-two interactions (54.74°). In this work, we expand upon this idea and demonstrate that with the use of appropriate affine transformations,[22] the anisotropies of the chemical shift and the quadrupolar coupling can be correlated in orthogonal dimensions, making the technique applicable to all half-integer quadrupolar nuclei. We refer to this experiment as correlation of anisotropies separated through echo refocusing (COASTER).

The COASTER experiment is a triple-to-single-quantum correlation with a coherence transfer pathway of $p = 0 \rightarrow +3 \rightarrow -1$ while the sample is spun at 70.12°. This pathway refocuses the second-rank quadrupolar anisotropy and chemical shift at different times in the 2D experiment. As illustrated in Figure 1, the quadrupolar anisotropy refocuses along the line $C_2^{[1]}t_1 + C_2^{[2]}t_2 = 0$, where $C_2^{[n]}$ is the second-order rank-two coefficient of the quadrupolar coupling in the $n$th dimension. Similarly, the chemical shift refocuses along the line $p^{[1]}t_1 + p^{[2]}t_2 = 0$, where $p^{[n]}$ is the coherence order in the $n$th dimension. The appropriate affine transformation for separating these interactions decomposes into a shearing transformation along the $\omega_1$ coordinate with ratio $\lambda_1$ followed by a scaling of $\omega_1$ by a factor $s_1$, after which $\omega_2$ is sheared and scaled by $\lambda_2$ and $s_2$, respectively (see Table 1 and the Supporting Information). Fourier transformation of the new time coordinates produces two frequency coordinates, which we label as $\omega_1'$(CSA) and $\omega_2'$(Q). The projection of the 2D COASTER spectrum onto the $\omega_2'$(Q) axis yields a 1D spectrum that depends only on the principal components of the quadrupolar-coupling tensor and is independent of the principal components of the chemical-shift tensor and the relative orientation of the two tensors. Similarly, the projection onto the $\omega_1'$(CSA) axis yields a 1D spectrum that contains only anisotropy from the chemical shift interaction and is independent of the second-rank anisotropic quadrupolar contribution to the transition frequency and the relative orientation of the two tensors. The isotropic chemical shift ($\delta_{cs}$) is obtained from the isotropic shifts found in the $\omega_1'$(CSA) and $\omega_2'$(Q) projections. This separation of anisotropies permits an accurate determination of the principal components of both the quadrupolar-coupling and chemical-shift tensors. The relative orientation of the two tensors is obtained by analyzing the pattern within the 2D COASTER spectrum. When the two tensors are diagonal in the same coordinate system, the 2D spectrum contains a triangular pattern, except when the asymmetry parameters for both tensors are zero ($\eta_{cs} = \eta_q = 0$), where the pattern in the 2D spectrum becomes a line. The vertices of the triangle correspond to the principal components of each tensor and establish which components are aligned. When the two tensors are not diagonal in the same coordinate system, an elliptical pattern appears in the 2D spectrum.

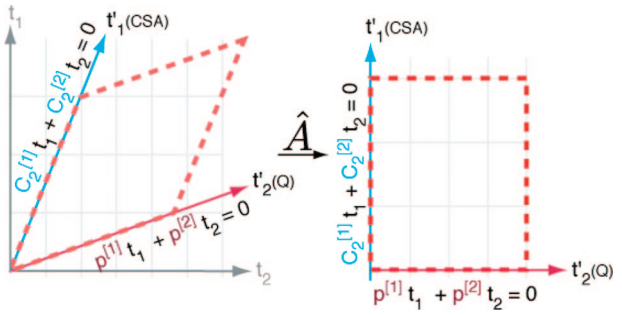


***Figure 1.*** Quadrupolar-coupling and chemical shift anisotropies are separated into orthogonal time domains after the application of an affine transformation using the shearing and scaling parameters given in Table 1.

***Table 1.*** Shearing Ratios ($\lambda$) and Scaling Factors ($s$) for the Two Dimensions in the COASTER Experiment

| $I$ | $\lambda_1$ | $s_1$ | $\lambda_2$ | $s_2$ |
|---|---|---|---|---|
| $^3/_2$ | 0 | 1 | $^1/_3$ | $^3/_4$ |
| $^5/_2$ | $^{15}/_8$ | $^8/_{23}$ | $^{23}/_9$ | $^9/_{32}$ |
| $^7/_2$ | $^{12}/_5$ | $^5/_{17}$ | $^{17}/_3$ | $^3/_{20}$ |
| $^9/_2$ | $^{21}/_8$ | $^8/_{29}$ | $^{29}/_3$ | $^3/_{32}$ |



10.1021/ja802865x CCC: $40.75 

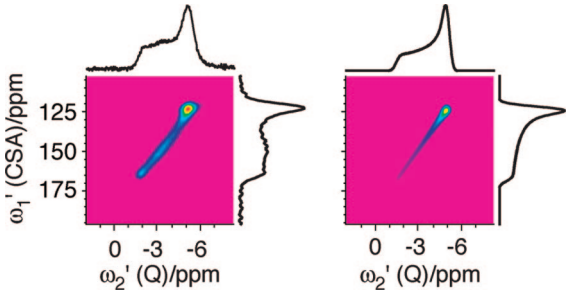


***Figure 2.*** (left) $^{63}$Cu COASTER spectrum of $K_3[Cu(CN)_4]$ at 9.4 T referenced to 1 M KCN/0.1 M CuCN, along with (right) a simulation using the parameter values $C_q = 1.1$ MHz, $\delta_{cs} = -49$ ppm, $\zeta_{cs} = 30$ ppm, and $\eta_q = \eta_{cs} = 0$.

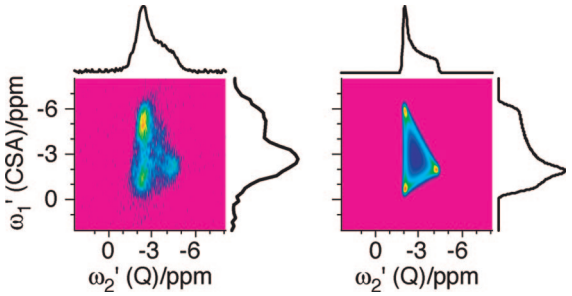


***Figure 3.*** (left) $^{59}$Co COASTER spectrum of $K_3[Co(CN)_6]$ at 9.4 T referenced to 1 M $K_3[Co(CN)_6]$, along with (right) a simulation using the parameter values $C_q = 6.2$ MHz, $\delta_{cs} = 14$ ppm, $\zeta_{cs} = -62$ ppm, $\eta_q = 1.0$, and $\eta_{cs} = 0.25$ and Euler angles $\alpha = 90°$ and $\beta = \gamma = 0°$.

If the chemical structure around a nucleus contains a symmetry axis, both the chemical shift and quadrupolar coupling often form axially symmetric tensors ($\eta_{cs} = \eta_q = 0$) that are aligned with the symmetry axis. For example, in $K_3[Cu(CN)_4]$, a model $Cu(CN)_4^{3-}$ structure that is popular for constructing supramolecular assemblies,[23] there is a $C_3$ axis along one of the Cu−CN bonds, and the largest principal components of both the chemical shift and quadrupolar coupling for $^{63}$Cu are aligned with this axis.[13] As shown in Figure 2, the $^{63}$Cu COASTER projections confirm that both tensors are symmetric, and the narrow ridge in the 2D spectrum indicates that the tensors are diagonal in the same axis system.

Quadrupolar couplings generally depend only on the electronic ground state, whereas the chemical shift also depends on excited electronic states. For example, in an analogous cobalt complex, $K_3[Co(CN)_6]$, there is a correlation between the $^{59}$Co CSA and the ratio of the quadrupolar coupling constant, $C_q$, to the d−d transition energy.[14] Thus, while the $^{59}$Co quadrupolar coupling is asymmetric ($\eta_q = 1$),[15] the CSA shows only a modest deviation from cylindrical symmetry ($\eta_{cs} = 0.25$). These differences in $\eta_q$ and $\eta_{cs}$ are observed in the 1D projections of the $^{59}$Co 2D COASTER spectrum in Figure 3, which also shows a triangular pattern in the 2D spectrum, indicating that the tensors are still diagonal in the same axis system with the coincident components evident from the vertices of the triangle.

In Figure 4, we show the $^{87}$Rb COASTER spectrum of $RbCrO_4$, where the appearance of an elliptical pattern indicates that the tensors are not diagonal in the same coordinate system. The simulation indicates that $\beta = 70°$, in agreement with previous measurements.[16] Components of the chemical-shift tensor generally align with the crystal axes for many Rb and Cs salts.[16] Thus, accurate measurement of the relative orientation allows one to determine the orientation of the quadrupolar-coupling tensor in the molecular frame without the need for ab initio calculations. Similar measurements could also be useful in carbonyl-containing systems

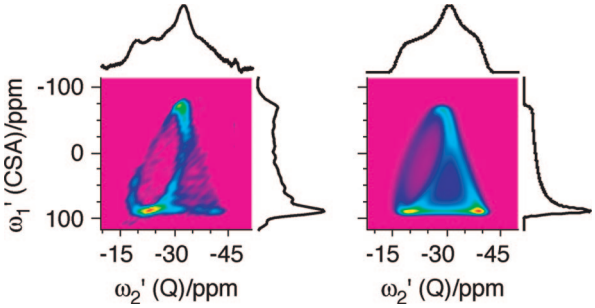


***Figure 4.*** (left) $^{87}$Rb COASTER spectrum of $RbCrO_4$ at 9.4 T referenced to 1 M $RbNO_3$, along with (right) a simulation using the parameter values $C_q = 3.5$ MHz, $\eta_q = 0.36$, $\delta_{cs} = -9$ ppm, $\zeta_{cs} = -110$ ppm, $\eta_{cs} = 0$, $\alpha = \gamma = 0°$, and $\beta = 70°$.

such as proteins, where the $^{17}$O quadrupolar-coupling tensor is always oriented along the carbonyl bond while substituent effects cause the chemical-shift tensor to rotate away from the bond.[17]

Since COASTER is performed at a fixed rotor axis, it can be implemented with minor modifications to most standard MAS probes. It should be noted that COASTER may be more appropriate for dilute or low-$\gamma$ nuclei, where the off-magic-angle spinning will not reintroduce strong dipolar couplings that could complicate interpretation. Finally, although COASTER will not resolve overlapping sites, it is possible to extend the ideas presented here into a 3D experiment for increased resolution.

**Acknowledgment.** This material is based upon work supported in part by the National Science Foundation under Grant CHE0616881.

**Supporting Information Available:** Transition frequencies, data processing, and additional simulated examples. This material is available free of charge via the Internet at http://pubs.acs.org.

## References

(1) Herzfeld, J.; Berger, A. E. *J. Chem. Phys.* **1980**, *73*, 6021–6030.
(2) Wu, Z. G.; Delaglio, F.; Tjandra, N.; Zhurkin, V. B.; Bax, A. *J. Biomol. NMR* **2003**, *26*, 297–315.
(3) Gregory, D. M.; Mehta, M. A.; Shiels, J. C.; Drobny, G. P. *J. Chem. Phys.* **1997**, *107*, 28–42.
(4) Pinheiro, T.; Watts, A. *Biochemistry* **1994**, *33*, 2451–2458.
(5) Meddour, A.; Berdague, P.; Hedli, A.; Courtieu, J.; Lesot, P. *J. Am. Chem. Soc.* **1997**, *119*, 4502–4508.
(6) Wu, C. H.; Ramamoorthy, A.; Gierasch, L. M.; Opella, S. J. *J. Am. Chem. Soc.* **1995**, *117*, 6148–6149.
(7) Tjandra, N.; Bax, A. *J. Am. Chem. Soc.* **1997**, *119*, 8076–8082.
(8) Fischer, M.; Zeng, L.; Pang, Y.; Hu, W. D.; Majumdar, A.; Zuiderweg, E. *J. Am. Chem. Soc.* **1997**, *119*, 12629–12642.
(9) Heller, J.; Laws, D. D.; Tomaselli, M.; King, D. S.; Wemmer, D. E.; Pines, A.; Havlin, R. H.; Oldfield, E. *J. Am. Chem. Soc.* **1997**, *119*, 7827–7831.
(10) Pervushin, K.; Riek, R.; Wider, G.; Wüthrich, K. *Proc. Natl. Acad. Sci. U.S.A.* **1997**, *94*, 12366–12371.
(11) Rowell, J. C.; Phillips, W. D.; Melby, L. R.; Panar, M. *J. Chem. Phys.* **1965**, *43*, 3442–3448.
(12) Cheng, J. T.; Edwards, J. C.; Ellis, P. D. *J. Phys. Chem.* **1990**, *94*, 553–561.
(13) Kroeker, S.; Wasylishen, R. E. *Can. J. Chem.* **1999**, *77*, 1962–1972.
(14) Chan, J.; Au-Yeung, S. *Annu. Rep. NMR Spectrosc.* **2000**, *41*, 1–54.
(15) Nielsen, U. G.; Jakobsen, H. J.; Skibsted, J. *Solid State Nucl. Magn. Reson.* **2001**, *20*, 23–34.
(16) Vosegaard, T.; Byriel, I. P.; Jakobsen, H. J. *J. Phys. Chem. B* **1997**, *101*, 8955–8958.
(17) Wu, G.; Yamada, K.; Dong, S.; Grondey, H. *J. Am. Chem. Soc.* **2000**, *122*, 4215–4216.
(18) Shore, J. S.; Wang, S. H.; Taylor, R. E.; Bell, A. T.; Pines, A. *J. Chem. Phys.* **1996**, *105*, 9412–9420.
(19) Medek, A.; Sachleben, J. R.; Beverwyk, P.; Frydman, L. *J. Chem. Phys.* **1996**, *104*, 5374–5383.
(20) Wang, S. H.; Xu, Z.; Baltisberger, J. H.; Bull, L. M.; Stebbins, J. F.; Pines, A. *Solid State Nucl. Magn. Reson.* **1997**, *8*, 1–16.
(21) Frydman, L.; Harwood, J. S. *J. Am. Chem. Soc.* **1995**, *117*, 5367–5368.
(22) Zwillinger, D. *CRC Standard Mathematical Tables and Formulae*; CRC Press: Boca Raton, FL, 1995; pp 265−266.
(23) Ibrahim, A. *J. Organomet. Chem.* **1998**, *556*, 1–9.

JA802865X

# Separating Chemical Shift and Quadrupolar Anisotropies with Multiple Quantum NMR Spectroscopy

Jason T. Ash, Nicole M. Trease, and Philip J. Grandinetti *

*Department of Chemistry, The Ohio State University, 120 W. 18th Avenue, Columbus, OH 43210-1173, USA*

Recieved Date: July 17, 2008. contact: *www.grandinetti.org/Contact*

In the first section of this supplement we derive the spatial and spin transition dependences of the chemical shift and quadrupolar contributions to the NMR transition frequency. In the second section we describe the shearing and scaling transformations used for the separation of the chemical shift and quadrupolar coupling frequency anisotropies in the COASTER experiment, provide a flow chart for processing COASTER data, and give some illustrative examples of how the 2D COASTER spectrum changes as the relative orientation of the chemical shift and quadrupolar coupling tensors is varied.

# 1 Transition Frequency

## 1.1 Chemical Shift Contribution

The first-order chemical shift contribution to the high field Hamiltonian, averaged over rapid sample rotation at an angle $\beta_R$, is written:

$$\hat{H}^{(1)}_{cs} = \hbar\omega_0 \left( \sigma + \sqrt{\frac{2}{3}} P_2(\cos\beta_R) A^{\{cs\}}_{2,0} \right) \hat{T}_{1,0}. \tag{1}$$

Here, $\omega_0$ is the Larmor frequency, $\sigma$ is isotropic shielding, $P_L(\cos\beta_R)$ is the Legendre polynomial of rank $L$, and $A^{\{cs\}}_{2,0}$ is an element of the rank two spherical tensor describing the spatial dependence of the chemical shift interaction in the rotor frame, which, in its principal axis system†, has the values of $\rho^{\{cs\}}_{2,0} = 3\zeta_{cs}/\sqrt{6}$, $\rho^{\{cs\}}_{2,\pm1} = 0$ and $\rho^{\{cs\}}_{2,\pm2} = \eta_{cs}\zeta_{cs}/2$ where $\zeta_{cs}$ is the shielding anisotropy and $\eta_{cs}$ is the shielding tensor asymmetry. This Hamiltonian leads to the first-order chemical shift contribution to the transition frequency of

$$\Omega_{cs} = \Upsilon^{\{cs\}}_{0,0} \cdot p \, + \, \Upsilon^{\{cs\}}_{2,0} \cdot p, \tag{2}$$

where $p$ is the coherence order, defined as $p = \langle m_s|\hat{T}_{1,0}|m_s\rangle - \langle m_r|\hat{T}_{1,0}|m_r\rangle = m_s - m_r$, and

$$\Upsilon^{\{cs\}}_{0,0} = \omega_0 \, \sigma \quad \text{and} \quad \Upsilon^{\{cs\}}_{2,0} = \omega_0 \sqrt{\frac{2}{3}} P_2(\cos\beta_R) A^{\{cs\}}_{2,0}. \tag{3}$$

## 1.2 Quadrupolar Coupling Contribution

The first-order quadrupolar contribution to the high field Hamiltonian is

$$\hat{H}^{(1)}_{q} = \hbar\omega_q A^{\{q\}}_{2,0} \hat{T}_{2,0}. \tag{4}$$

†When the principal axis system (PAS) of the chemical shift and quadrupolar interactions are not coincident, it is helpful to transform into a common axis system. If one chooses the PAS of the quadrupolar coupling interaction as the common coordinate system, then the tensor components of the chemical shift interaction will be given by:

$$A^{\{cs\}\prime}_{l,k} = \sum_{k'=-l}^{l} \mathcal{D}^{(l)}_{k,k'}(\Lambda) A^{\{cs\}}_{l,k'} = \sum_{k'=-l}^{l} e^{-ik\alpha} d^{(l)}_{k,k'}(\beta) e^{-ik'\gamma} A^{\{cs\}}_{l,k'},$$

before using in Eqs. (2) and (7). Here $\Lambda$ are the Euler angles $(\alpha, \beta, \gamma)$ describe the relative orientation between the principal axis systems of the two interactions.

Here, $\omega_q = 6\pi C_q/2I(2I-1)$, where $C_q$ is the quadrupolar coupling constant and $A^{\{q\}}_{2,0}$ is an element of the rank two spherical tensor describing the spatial dependence of the quadrupolar interaction in the rotor frame, which, in its principal axis system, has the values of $\rho^{\{q\}}_{2,0} = 1/\sqrt{6}$, $\rho^{\{q\}}_{2,\pm1} = 0$ and $\rho^{\{q\}}_{2,\pm2} = \eta_q/6$, where $\eta_q$ is the quadrupolar tensor asymmetry. For many spin $I > 1/2$ nuclei the quadrupolar coupling is strong enough to require the inclusion of a second-order correction, which, averaged over rapid sample rotation, is given by[‡]

$$\hat{H}^{(2)}_q = -\frac{\hbar\omega_q^2}{\omega_0} \sum_{L=0,2,4} P_L(\cos\beta_R)\mathcal{A}^{\{q\}}_{L,0} \sum_{J=1,3} a_{L,J}\ \hat{\mathcal{T}}_{J,0}. \tag{5}$$

Here the tensor $\mathcal{A}^{\{q\}}_{L,n}$ is related to the principal values of the $A^{\{q\}}_{L,n}$ tensor by

$$\mathcal{A}^{\{q\}}_{L,n} = \sum_{n'=-L}^{L} \mathcal{D}^{(L)}_{n',n}(\Omega_q)\,\sigma^{\{q\}}_{L,n'},$$

where

$$\sigma^{\{q\}}_{L,n} = \sum_k \langle L\ n\,|2\ 2\ k\ n-k\rangle\,\rho^{\{q\}}_{2,k}\ \ \rho^{\{q\}}_{2,n-k}. \tag{6}$$

From Eq. (6) we obtain the relationships:

$$\sigma^{\{q\}}_{0,0} = \frac{1}{6\sqrt{5}}\left(\frac{\eta_q^2}{3}+1\right),$$

$$\sigma^{\{q\}}_{2,0} = \frac{1}{6}\sqrt{\frac{2}{7}}\left(\frac{\eta_q^2}{3}-1\right), \quad \sigma^{\{q\}}_{2,\pm2} = \frac{\eta_q}{3\sqrt{21}},$$

$$\sigma^{\{q\}}_{4,0} = \frac{1}{\sqrt{70}}\left(\frac{\eta_q^2}{18}+1\right), \quad \sigma^{\{q\}}_{4,\pm2} = \frac{\eta_q}{6\sqrt{7}}, \quad \sigma^{\{q\}}_{4,\pm4} = \frac{\eta_q^2}{36}.$$

The coefficients $a_{L,J}$ are given by

$$a_{L,J} = 2\sum_{k>0} \frac{\langle L\,0|2\,2\,k\ -k\rangle\,\langle J\,0|2\,2\,k\ -k\rangle}{k},$$

and, using the Wigner-Eckert theorem, the $\hat{\mathcal{T}}_{l,k}$ are related to our originally defined irreducible tensor operators, $\hat{T}_{l,k}$, according to:

$$\hat{\mathcal{T}}_{1,0} = \sqrt{\frac{2}{5}}\,[I(I+1)-3/4]\,\hat{T}_{1,0},$$

and

$$\hat{\mathcal{T}}_{3,0} = -2\,\hat{T}_{3,0}.$$

The symmetric ($-m \leftrightarrow m$) transitions, which are employed in the COASTER experiment, are unaffected by the first order quadrupolar Hamiltonian. Thus, the most significant contribution from the quadrupolar interaction to the symmetric transition frequencies comes from the second-order correction, where we obtain

$$\Omega_q = -\frac{\omega_q^2}{\omega_0} \sum_{L=0,2,4} P_L(\cos\beta_R)\mathcal{A}^{\{q\}}_{L,0}\cdot C_L, \tag{7}$$

with

$$C_L = \sum_{J=1,3} a_{L,J}\Big\{\langle m_s|\hat{\mathcal{T}}_{J,0}|m_s\rangle - \langle m_r|\hat{\mathcal{T}}_{J,0}|m_r\rangle\Big\}. \tag{8}$$

[‡]for more details, see P. Grandinetti, *Solid State Nucl. Mag. Reson.*, **23**, 1-13 (2003).

The $C_L$ describe the spin transition dependent part of the second-order quadrupolar contribution to the transition frequency and play a role analogous to $p$, but are more complex functions of $I$, $m_r$, and $m_s$. Thus, by defining

$$\Upsilon_{L,0}^{\{q\}} = \frac{\omega_q^2}{\omega_0} P_L(\cos\beta_R)\, \mathcal{A}_{L,0}^{\{q\}}, \tag{9}$$

we can expand the second-order quadrupolar contribution to the transition frequency into three components having different products of spatial and spin transition dependences:

$$\Omega_q \;=\; -\Upsilon_{0,0}^{\{q\}} \cdot C_0 \;-\; \Upsilon_{2,0}^{\{q\}} \cdot C_2 \;-\; \Upsilon_{4,0}^{\{q\}} \cdot C_4. \tag{10}$$

# 2 COASTER

The frequency of a symmetric transition in a static sample experiencing both the chemical shift and quadrupolar interactions will depend on five components,

$$\Omega_{\text{static}} = \Upsilon_{0,0}^{\{cs\}} \cdot p \;-\; \Upsilon_{0,0}^{\{q\}} \cdot C_0 \;+\; \Upsilon_{2,0}^{\{cs\}} \cdot p \;-\; \Upsilon_{2,0}^{\{q\}} \cdot C_2 \;-\; \Upsilon_{4,0}^{\{q\}} \cdot C_4, \tag{11}$$

each involving different products of spatial and spin transition dependences. The lineshape of a site in a polycrystalline sample with this frequency dependence would depend on eight parameters: $C_q$, $\eta_q$, $\sigma$, $\zeta_{cs}$, $\eta_{cs}$, and the three Euler angles, $\alpha$, $\beta$, and $\gamma$, for the relative orientation of the quadrupolar and chemical shift tensors. While magic-angle spinning (MAS) does not remove all anisotropy for quadrupolar nuclei with second-order broadenings, it does eliminate the second rank anisotropies, that is, $\Upsilon_{2,0}^{\{cs\}} = \Upsilon_{2,0}^{\{q\}} = 0$, and then the frequency depends only on three components:

$$\Omega_{\text{MAS}} = \Upsilon_{0,0}^{\{cs\}} \cdot p \;-\; \Upsilon_{0,0}^{\{q\}} \cdot C_0 \;-\; \Upsilon_{4,0}^{\{q\}} \cdot C_4. \tag{12}$$

Thus, the MAS lineshape of a site depends only on three parameters: $C_q$, $\eta_q$, and $\sigma$. In other words, the dependence on the chemical shift anisotropy, $\zeta_{cs}$, $\eta_{cs}$, and the relative tensor orientation, $\alpha$, $\beta$, and $\gamma$, are removed from the spectrum. This simplification, or elimination of five out of eight parameters, allows a more accurate and precise determination of $C_q$, $\eta_q$, and $\sigma$ from a MAS spectrum. Until now, there existed no analogous experiment for obtaining a spectrum with the dependences on the quadrupolar anisotropy and the relative tensor orientation suppressed leaving only isotropic shifts and the chemical shift anisotropy. The COASTER experiment described here not only provides this spectrum, but also provides a spectrum that depends only on $C_q$, $\eta_q$, and $\sigma$, even though COASTER does not employ MAS conditions. These two spectra are the one-dimensional projections of the two-dimensional COASTER spectrum. Additionally, information about the relative tensor orientation, that is, $\alpha$, $\beta$, and $\gamma$, is available within the full two-dimensional COASTER spectrum.

The COASTER experiment achieves this simplification by spinning at a rotor angle of 70.12°, where $\Upsilon_{4,0}^{\{q\}} = 0$ and the transition frequency is given by

$$\Omega_{70.12^\circ} = \Upsilon_{0,0}^{\{cs\}} \cdot p - \Upsilon_{0,0}^{\{q\}} \cdot C_0 + \Upsilon_{2,0}^{\{cs\}} \cdot p - \Upsilon_{2,0}^{\{q\}} \cdot C_2. \tag{13}$$

The anisotropy of the chemical shift and second-order quadrupolar coupling are contained with the terms $\Upsilon_{2,0}^{\{cs\}}$ and $\Upsilon_{2,0}^{\{q\}}$, respectively. In the COASTER experiment a two-dimensional signal correlating triple quantum evolution with single quantum evolution given by

$$S(t_1,t_2) = \exp\left\{ i\left( \Omega_{iso}^{[1]} + \Upsilon_{2,0}^{\{cs\}} \cdot p^{[1]} - \Upsilon_{2,0}^{\{q\}} \cdot C_2^{[1]} \right) t_1 \right\} \exp\left\{ i\left( \Omega_{iso}^{[2]} + \Upsilon_{2,0}^{\{cs\}} \cdot p^{[2]} - \Upsilon_{2,0}^{\{q\}} \cdot C_2^{[2]} \right) t_2 \right\}, \tag{14}$$

is obtained, where

$$\Omega_{iso}^{[n]} = \Upsilon_{0,0}^{\{cs\}} \cdot p^{[n]} - \Upsilon_{0,0}^{\{q\}} \cdot C_0^{[n]}. \tag{15}$$

Here $p^{[n]}$ and $C_L^{[n]}$ are the spin transition dependent coefficients during the $n$th time dimension. By rearranging this signal to the form

$$S(t_1,t_2) = \exp\left\{ i\left( \Omega_{iso}^{[1]} t_1 + \Omega_{iso}^{[2]} t_2 \right) \right\} \exp\left\{ i\Upsilon_{2,0}^{\{cs\}} \left( p^{[1]} t_1 + p^{[2]} t_2 \right) \right\} \exp\left\{ -i\Upsilon_{2,0}^{\{q\}} \left( C_2^{[1]} t_1 + C_2^{[2]} t_2 \right) \right\}, \tag{16}$$

we see that the chemical shift and quadrupolar anisotropies, $\Upsilon_{2,0}^{\{cs\}}$ and $\Upsilon_{2,0}^{\{q\}}$, respectively, can be separated into orthogonal dimensions if the time coordinates are redefined according to

$$\underbrace{\begin{pmatrix} t_1 \\ \\ t_2 \end{pmatrix}}_{\mathbf{t}} = \underbrace{\begin{pmatrix} \dfrac{C_2^{[2]}}{C_2^{[2]}-C_2^{[1]}} & \dfrac{p^{[2]}}{p^{[2]}-p^{[1]}} \\ -\dfrac{C_2^{[1]}}{C_2^{[2]}-C_2^{[1]}} & -\dfrac{p^{[1]}}{p^{[2]}-p^{[1]}} \end{pmatrix}}_{\mathcal{A}} \underbrace{\begin{pmatrix} t_1' \\ \\ t_2' \end{pmatrix}}_{\mathbf{t}'}. \tag{17}$$

Using these definitions, one obtains

$$p^{[1]}t_1 + p^{[2]}t_2 = -\frac{p^{[2]}C_2^{[1]} - p^{[1]}C_2^{[2]}}{C_2^{[2]}-C_2^{[1]}}t_1' \quad \text{and} \quad C_2^{[1]}t_1 + C_2^{[2]}t_2 = \frac{p^{[2]}C_2^{[1]} - p^{[1]}C_2^{[2]}}{p^{[2]}-p^{[1]}}t_2', \tag{18}$$

and the signal as a function of the transformed time coordinates becomes

$$S'(t_1',t_2') = \exp\{i\Omega'^{[1]}_{iso}t_1'\}\exp\{i\Omega'^{[2]}_{iso}t_2'\}\exp\left\{-i\Upsilon_{2,0}^{\{cs\}}\left(\frac{p^{[2]}C_2^{[1]} - p^{[1]}C_2^{[2]}}{C_2^{[2]}-C_2^{[1]}}\right)t_1'\right\}\exp\left\{-i\Upsilon_{2,0}^{\{q\}}\left(\frac{p^{[2]}C_2^{[1]} - p^{[1]}C_2^{[2]}}{p^{[2]}-p^{[1]}}\right)t_2'\right\}, \tag{19}$$

where

$$\Omega'^{[1]}_{iso} = \frac{C_2^{[2]}\Omega_{iso}^{[1]} - C_2^{[1]}\Omega_{iso}^{[2]}}{C_2^{[2]}-C_2^{[1]}} \quad \text{and} \quad \Omega'^{[2]}_{iso} = \frac{p^{[2]}\Omega_{iso}^{[1]} - p^{[1]}\Omega_{iso}^{[2]}}{p^{[2]}-p^{[1]}}. \tag{20}$$

This transformation separates the chemical shift and quadrupolar anisotropies, with $\Upsilon_{2,0}^{\{cs\}}$ evolving only during $t_1'$ and $\Upsilon_{2,0}^{\{q\}}$ only during $t_2'$. Note that each column of $\mathcal{A}$ sums to unity. This can be understood by envisioning $t_1$ and $t_2$ as a simple weighted average of two new coordinates $t_1'$ and $t_2'$. The transformation from the original (unprimed) coordinates to the new (primed) coordinates, is obtained by inverting Eq. (17):

$$\underbrace{\begin{pmatrix} t_1' \\ \\ t_2' \end{pmatrix}}_{\mathbf{t}'} = \underbrace{\begin{pmatrix} \dfrac{p^{[1]}\left(C_2^{[2]}-C_2^{[1]}\right)}{p^{[1]}C_2^{[2]}-p^{[2]}C_2^{[1]}} & \dfrac{p^{[2]}\left(C_2^{[2]}-C_2^{[1]}\right)}{p^{[1]}C_2^{[2]}-p^{[2]}C_2^{[1]}} \\ -\dfrac{C_2^{[1]}\left(p^{[2]}-p^{[1]}\right)}{p^{[1]}C_2^{[2]}-p^{[2]}C_2^{[1]}} & -\dfrac{C_2^{[2]}\left(p^{[2]}-p^{[1]}\right)}{p^{[1]}C_2^{[2]}-p^{[2]}C_2^{[1]}} \end{pmatrix}}_{\mathcal{A}^{-1}} \underbrace{\begin{pmatrix} t_1 \\ \\ t_2 \end{pmatrix}}_{\mathbf{t}}. \tag{21}$$

The corresponding frequency domain transformation is related to Eq. (21) by

$$\begin{pmatrix} \omega_1', & \omega_2' \end{pmatrix} = \begin{pmatrix} \omega_1, & \omega_2 \end{pmatrix} \underbrace{\begin{pmatrix} \dfrac{C_2^{[2]}}{C_2^{[2]}-C_2^{[1]}} & \dfrac{p^{[2]}}{p^{[2]}-p^{[1]}} \\ -\dfrac{C_2^{[1]}}{C_2^{[2]}-C_2^{[1]}} & -\dfrac{p^{[1]}}{p^{[2]}-p^{[1]}} \end{pmatrix}}_{\left(\mathcal{A}^{-1}\right)^{-1}=\mathcal{A}}. \tag{22}$$

This type of transformation can be implemented as a product of shearing and scaling transformations. We adopt the following convention for decomposing the transformation matrix $\mathcal{A}$ into shearing and scaling transformations

$$\mathcal{A} = \underbrace{\begin{pmatrix} 1 & 0 \\ \\ \lambda_1 & 1 \end{pmatrix}}_{\text{shear } \omega_1} \underbrace{\begin{pmatrix} s_1 & 0 \\ \\ 0 & 1 \end{pmatrix}}_{\text{scale } \omega_1} \underbrace{\begin{pmatrix} 1 & \lambda_2 \\ \\ 0 & 1 \end{pmatrix}}_{\text{shear } \omega_2} \underbrace{\begin{pmatrix} 1 & 0 \\ \\ 0 & s_2 \end{pmatrix}}_{\text{scale } \omega_2}. \tag{23}$$

The solution to these equations is given by

$$\lambda_1 = -\frac{C_2^{[1]}}{C_2^{[2]}}, \quad s_1 = \frac{C_2^{[2]}}{C_2^{[2]} - C_2^{[1]}}, \quad \lambda_2 = \frac{p^{[2]}(C_2^{[2]} - C_2^{[1]})}{p^{[2]}C_2^{[1]} - p^{[1]}C_2^{[2]}}, \text{ and } s_2 = \frac{p^{[2]}C_2^{[1]} - p^{[1]}C_2^{[2]}}{(p^{[2]} - p^{[1]})C_2^{[2]}}. \tag{24}$$

These expressions were used to determine the shearing and scaling ratios listed in Table 1 of the main article for all half-integer spin values. In Fig. 1 is a flowchart describing the transformation of the raw COASTER 2D time domain data (Fig. 1A) into the 2D COASTER spectrum (Fig. 1I) using these scaling and shearing parameters.

In Fig. 2 are simulated 2D COASTER spectra showing the effect of the changing quadrupolar coupling and chemical shift asymmetry parameters in the case where the quadrupolar coupling and chemical shift tensors have the same principal axis systems. Generally, whenever the two tensors are diagonal in the same coordinate system, the 2D spectrum will form a triangular pattern, except in the case with $\eta_q = \eta_{cs} = 0$, where the resulting pattern is a line in the two-dimensional spectrum. The vertices of the triangle correspond to the principle components of the two tensors and unambiguously establish which components are aligned.

The sensitivity of the COASTER spectrum to the relative orientation of the two tensors is shown in the simulations of Fig. 3. Notice that the projections onto the individual axes are unchanged as the chemical shift and quadrupolar coupling tensors are fixed. The principal components of the chemical shift and quadrupolar coupling tensors can be determined solely by analysis of the corresponding one-dimensional projections, which are independent of the relative orientation of the two tensors. In contrast, the relative orientation of the two tensors can be obtained by analysis of the pattern contained with the 2D COASTER spectrum. In these examples, one Euler angle is varied from 90° to 0°, while the other two angles are fixed at 90°. Note that when the Euler angles are all multiples of 90°, the spectrum forms a triangular pattern, as the two tensors are diagonal in a common coordinate system. When an Euler angle is not a multiple of 90°, however, an elliptical pattern appears in the 2D spectrum.

## 2.1 Experimental Details

All samples used in this study were purchased from Strem and used without further purification with the exception of $K_3Cu(CN)_4$, which was crystallized from an aqueous solution containing KCN and CuCN. Experiments were performed at 9.4 T on a Bruker Avance 400 spectrometer using a 4 mm CMX MAS probe spinning at 15 kHz. The fixed rotor axis of 70.1±0.5° was calibrated by observing the residual quadrupolar splitting of $^2$H in deuterated hexamethylbenzene. Cu-63 spectra were acquired at 106.25 MHz and referenced to an aqueous solution containing $Cu(CN)_4^{3-}$ ions by preparing an aqueous solution of CuCN with a large excess of KCN. Spectra of Rb-87 (I=3/2) were recorded at 131.07 MHz and referenced to an aqueous solution of $RbNO_3$. Spectra of Co-59 (I=7/2)were referenced to a solution of $K_3[Co(CN)_6]$. The spectra of $K_3[Co(CN)_6]$ were acquired at a frequency of 95.05 MHz, while the large chemical shift of $Na_3[Co(NO_2)_6]$ require a Larmor frequency of 95.78 MHz. The pulse sequence utilized in this experiment is identical to the three pulse shifted echo MQ-MAS sequence[§]. For excitation and conversion of triple quantum coherence, hard pulses of $\nu_1$=200 kHz were employed with durations optimized for the particular sample, but typically of typically 3 $\mu$s and 1 $\mu$s, respectively. The last pulse is a selective ($\nu_1$ =20 kHz) $\pi$ pulse on the central transition. The recycle delay was 1s and each spectrum required 24 hours of spectrometer time to acquire.

### Note

We thank a reviewer for pointing out that it may be possible to develop the CQ-PRODI experiment of Vosegaard and Massiot[¶] into a method for obtaining the same information from quadrupolar nuclei in solids.

[§]Massiot *et al.*, *Solid State NMR*, **6**, 73 (1996)

[¶]Thomas Vosegaard and Dominique Massiot, "High-resolution two-dimensional NMR spectra of half-integer-spin quadrupolar nuclei from one-dimensional projections", *Chem. Phys. Lett.*, **437**, 120-125 (2007).

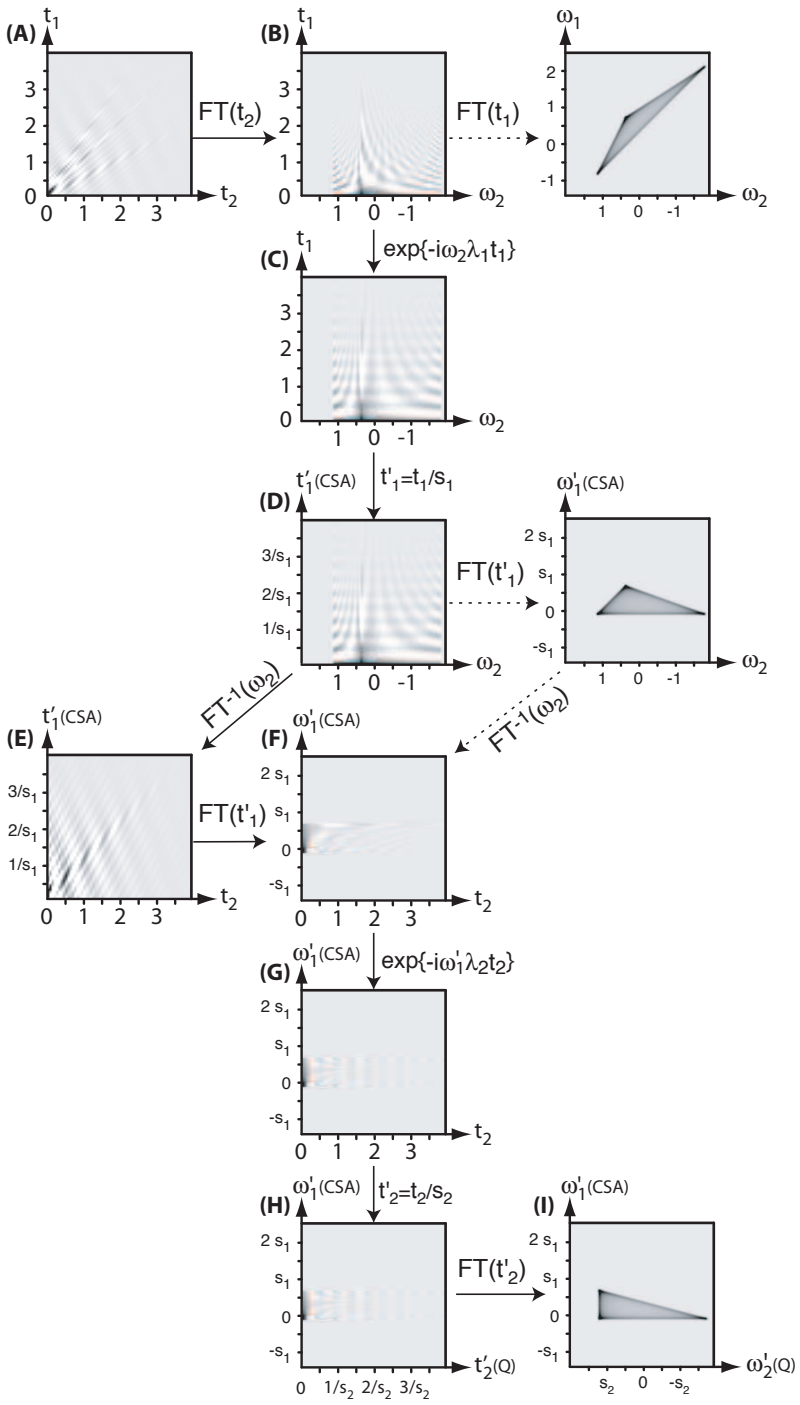


Figure 1: Flow chart for transforming the raw COASTER 2D time domain data **(A)** into the 2D COASTER spectrum **(I)**. The $\lambda_1$ shear is performed by a Fourier transformation of **(A)** with respect to $t_2$ followed by a $t_1$ dependent first-order phase correction of $\exp\{-i\omega_2\lambda_1 t_1\}$ applied to the $\omega_2$ dimension to obtain **(C)**. **(D)** is obtained after scaling the $t_1$ dimension by $1/s_1$. An inverse Fourier transformation with respect to $\omega_2$ dimension creates the $(t'_1, t_2)$ domain data of **(E)**. The $\lambda_2$ shear is performed by a Fourier transformation of **(E)** with respect to $t'_1$ followed by a $t_2$ dependent first-order phase correction of $\exp\{-i\omega'_1\lambda_2 t_2\}$ applied to the $\omega'_1$ dimension to obtain **(G)**. **(H)** is obtained after scaling the $t_2$ dimension by $1/s_2$. Fourier transform with respect to $t'_2$ results in final 2D COASTER spectrum, **(I)**.

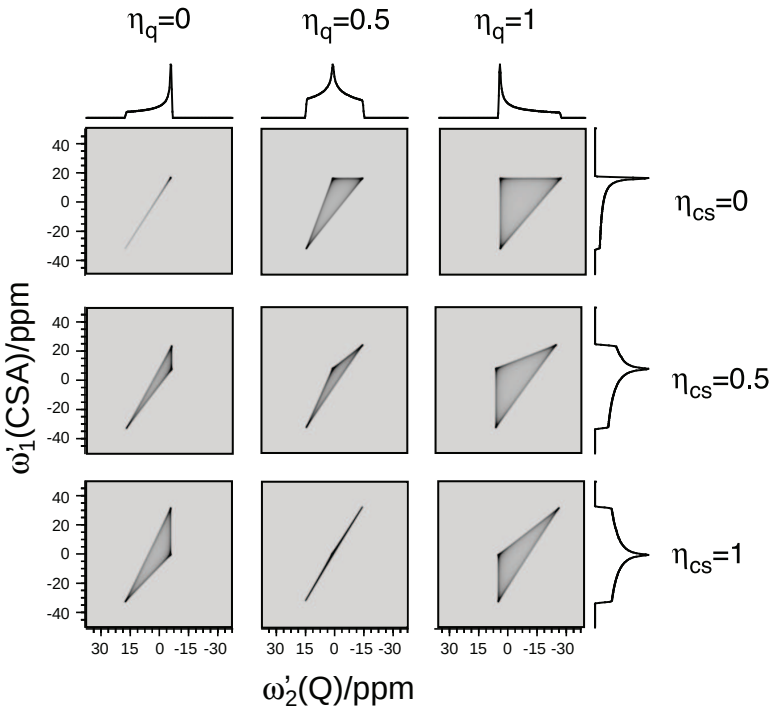


Figure 2: Comparison of simulated 2D COASTER spectra showing the effect of the changing quadrupolar coupling and chemical shift asymmetry parameters in the case where the quadrupolar coupling and chemical shift tensors have the same principal axis systems. Other simulation parameters included $I = 3/2$, $\omega_0 = 100$ MHz, $C_q = 3$ MHz, $\sigma = 0$ ppm and $\zeta_{cs} = 33$ ppm. The one-dimensional projections onto the quadrupolar anisotropy axis, $\omega_2'$(Q), are the same for each $\eta_q$ value. Similarly, the one-dimensional projections onto the chemical shift anisotropy axis, $\omega_1'$(CSA), is the same for each $\eta_{cs}$ value.

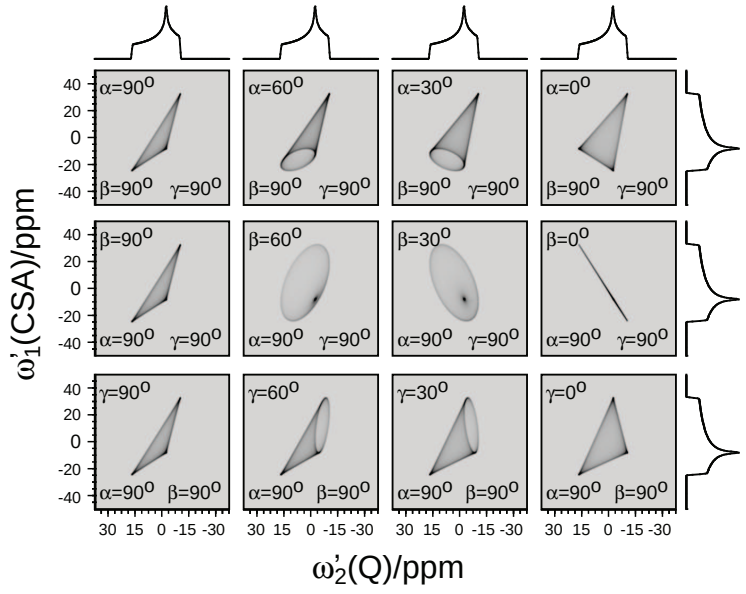


Figure 3: Comparison of simulated COASTER spectra showing the effect of the relative orientation on the two-dimensional spectrum. Other simulation parameters included $I = 3/2$, $\omega_0 = 100$ MHz, $C_q = 3$ MHz, $\eta_q = 0.25$, $\sigma = 0$ ppm, $\zeta_{cs} = 33$ ppm, and $\eta_{cs} = 0.5$. Again, note that the projection onto each axis remains unchanged as the relative orientation of the quadrupolar coupling and chemical shift tensors change.